**Supporting Information**

# Interfacial Structure and Proton Conductivity of Nafion at the Pt-deposited Surface

Yutaro Ono and Yuki Nagao*

School of Materials Science, Japan Advanced Institute of Science and Technology, 1-1

Asahidai, Nomi, Ishikawa 923-1292 Japan

Tel; +81761 51 1541; *E-mail: ynagao@jaist.ac.jp

**Contents**

## S1. AFM image of the cross-section of Pt-deposited surface

The thickness of the Pt thin film was c.a. 15-20 nm [Figure S1] determined by the atomic force microscopy (AFM, VN-8000; Keyence Co.).

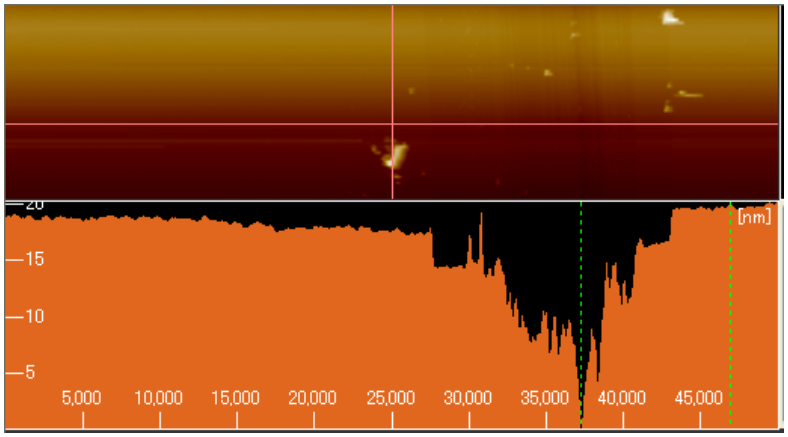


**Figure S1 AFM image of the cross-section of Pt/$SiO_2$ surface**

## S2. FT-IR single beam spectra of different angle

Figure S2 shows the single-beam spectra with the different incident angles. The intensity of the single-beam in the case of thicker Pt-deposited substrate was almost zero. However, the intensity for the thin Pt-deposited MgO (Figure S2(b)) was only 10% lower than that of the bare MgO substrate (Figure S2(a)). Each spectrum had a similar shape in the case of Pt-deposited and bare MgO substrates. The intensity of the single beam spectra gradually decreased when the angle of incident decreased from 38° to 8°. Therefore, we inferred that this p-MAIRS technique is applicable with the Pt-deposited surface. To confirm the reproducibility for the Pt deposition, Figure S2(c) shows the Pt-deposited MgO surface of three different samples at 38°. Three different

samples show similar spectra. The single beam spectra of the $SiO_2$ showed different spectra compared to the MgO substrate. Because $SiO_2$ has a low IR transmittance (Figure S2(f)) due to the large absorption band at less than ca. 2100 $cm^{-1}$. The intensity from 4000 to 2200 $cm^{-1}$ in the case of thin Pt-deposited $SiO_2$ (Figure S2(e)) was 4 to 10 % decrease compared with the bare $SiO_2$ substrate (Figure S2(d)). This value is relatively close to the Pt-deposited MgO.

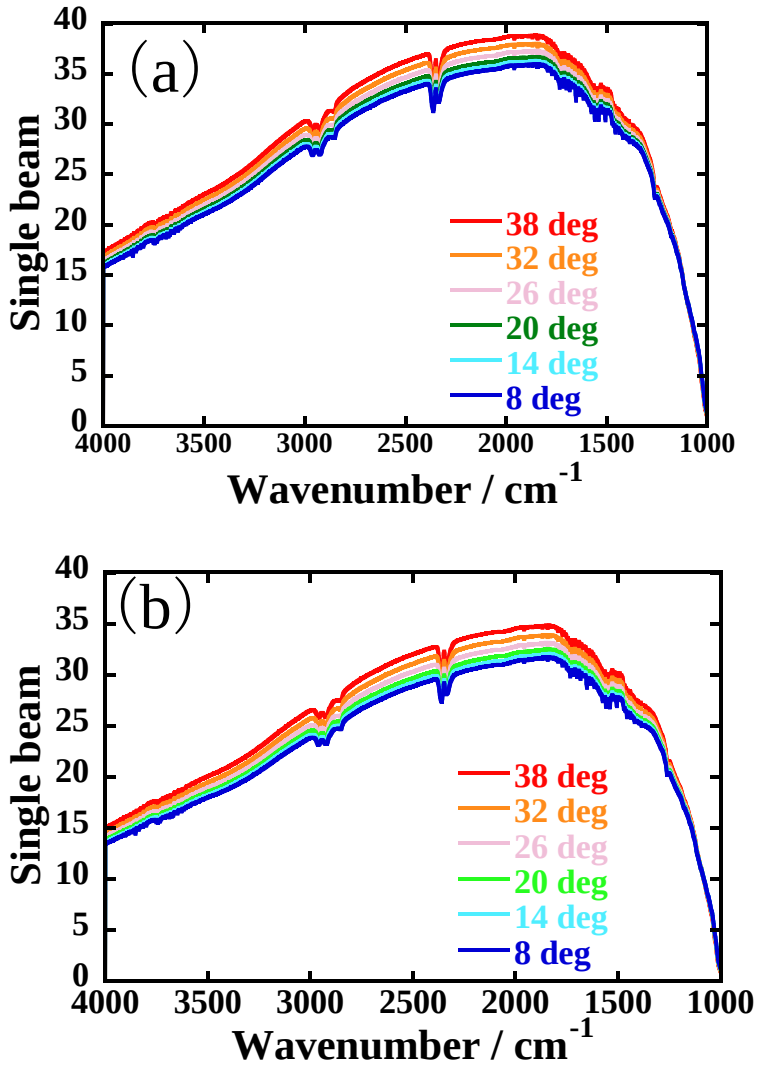

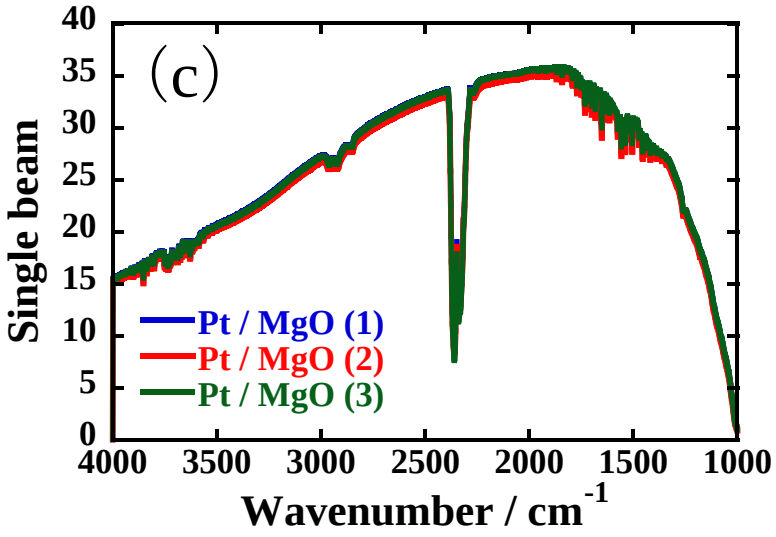
(c)
Single beam
Wavenumber / cm-1
Pt / MgO (1)
Pt / MgO (2)
Pt / MgO (3)

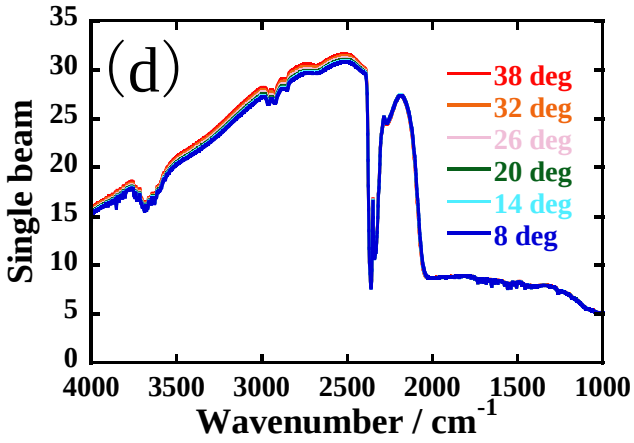
(d)
Single beam
Wavenumber / cm-1
38 deg
32 deg
26 deg
20 deg
14 deg
8 deg

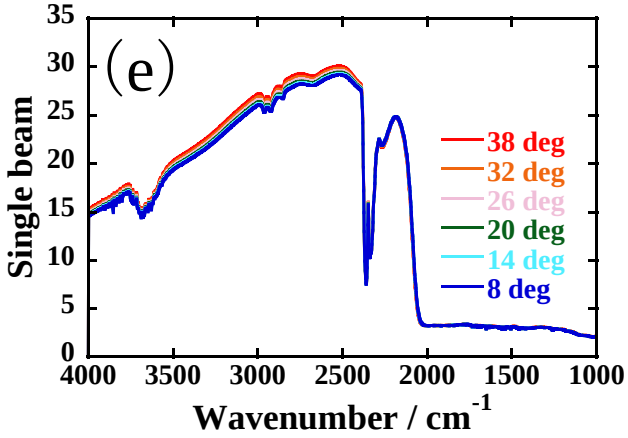
(e)
Single beam
Wavenumber / cm-1
38 deg
32 deg
26 deg
20 deg
14 deg
8 deg

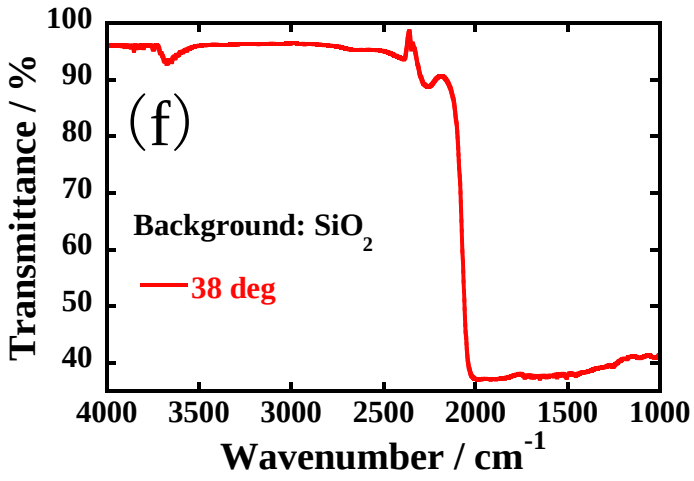


Figure S2 Single beam spectra of different angle and Transmission spectrum. (a) MgO substrate (b) Pt-deposited MgO surface (c) Pt-deposited MgO surface for three different samples at 38 degree (d) $SiO_2$ substrate (e) and (f) Pt-deposited $SiO_2$ surface.

**S3. Humidity dependence of the resistance for Nafion / Pt and Pt / $SiO_2$**

Figure S3 shows the RH dependence of the resistance of Pt-deposited surface on $SiO_2$ substrate. The resistance of the Pt-deposited surface was $10^{11}$ ohm and did not depend on the RH. In contrast, the resistance of the 20-nm-thick Nafion thin film deposited on Pt-deposited surface was highly dependent on the RH. The resistance of the Pt-deposited was one order of magnitude higher than that of the Nafion thin films in the whole RH region. Therefore the proton conductivity can be evaluated compared to the Pt electronic conductivity.

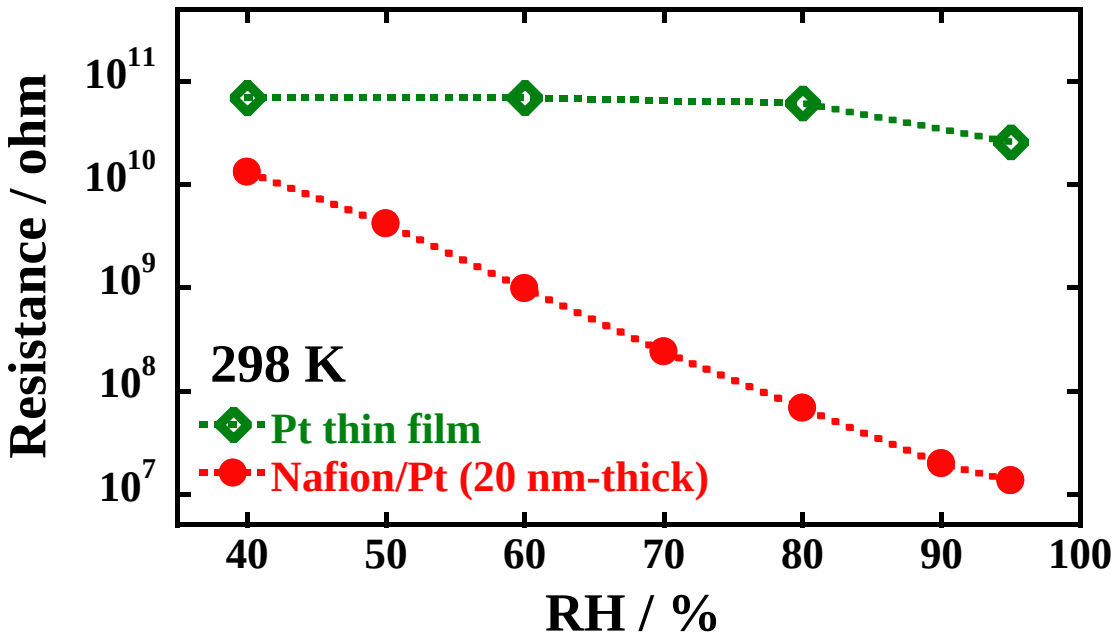


Figure S3 Humidity dependence (RH) of the resistance obtained directly from the impedance measurement.

**S4 XPS spectra of Pt 4f and Si 2p electrons from Pt / $SiO_2$ substrate**

Figure S4 shows the XPS spectra of Pt 4f and Si 2p electrons for the Pt / $SiO_2$ substrate. The binding energies of Pt $4f_{7/2}$, $4f_{5/2}$ electron peaks were found to be 71.5 eV and 74.7 eV, respectively.

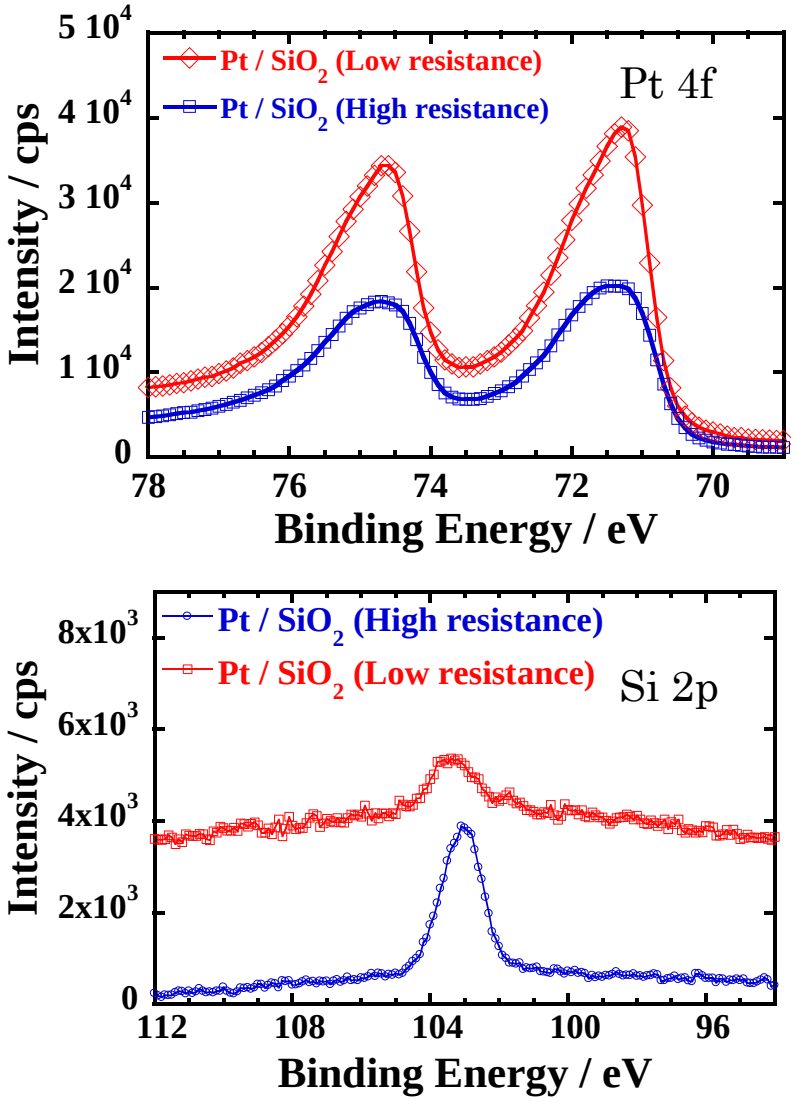


Figure S4 XPS spectra of Pt 4f and Si 2p electrons from Pt / $SiO_2$ substrate

**S5 Curve-fitted XPS spectra for the Pt 4f**

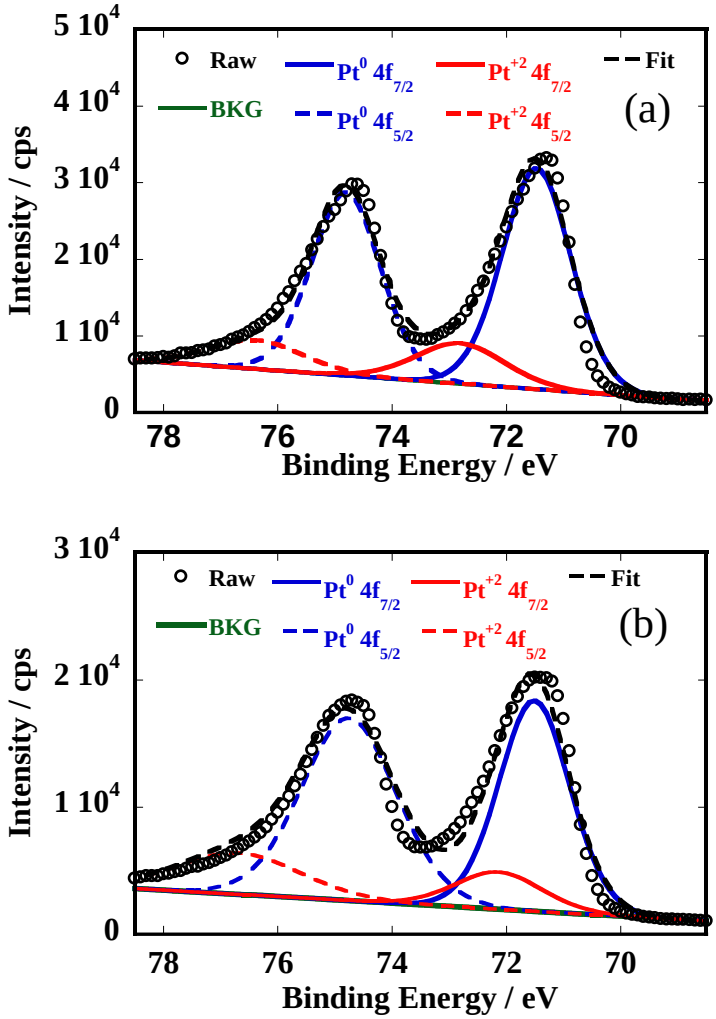


Figure S5 Curve-fitted XPS spectra for the Pt 4f core binding energy region of (a) Low, (b) High resistance.

Table S1 Relative peak area from curve-fitted XPS spectra

| | $Pt^{+0}\,4f_{5/2}$ | $Pt^{+2}\,4f_{5/2}$ |
|---|---|---|
| (a) | 85 % | 15 % |
| (b) | 75 % | 25% |

**S6. AFM images of Pt and bare surface.**

The surface morphology of the bare surface and Pt-deposited surface was obtained using AFM. Figure S6 shows the topographic AFM images of the bare surface and Pt-deposited surface. Each image represents in the dimension 10 μm × 10 μm. The smooth surface images were obtained from both bare MgO and $SiO_2$ surfaces in Figure S6(a) and S6(b), respectively. In contrast, the rougher surfaces compared to bare surface were observed in both Pt-deposited MgO and $SiO_2$ surfaces as shown in Figure S6(c) and S6(d). These results support that the Pt-deposited surface has the island morphology on both substrates.

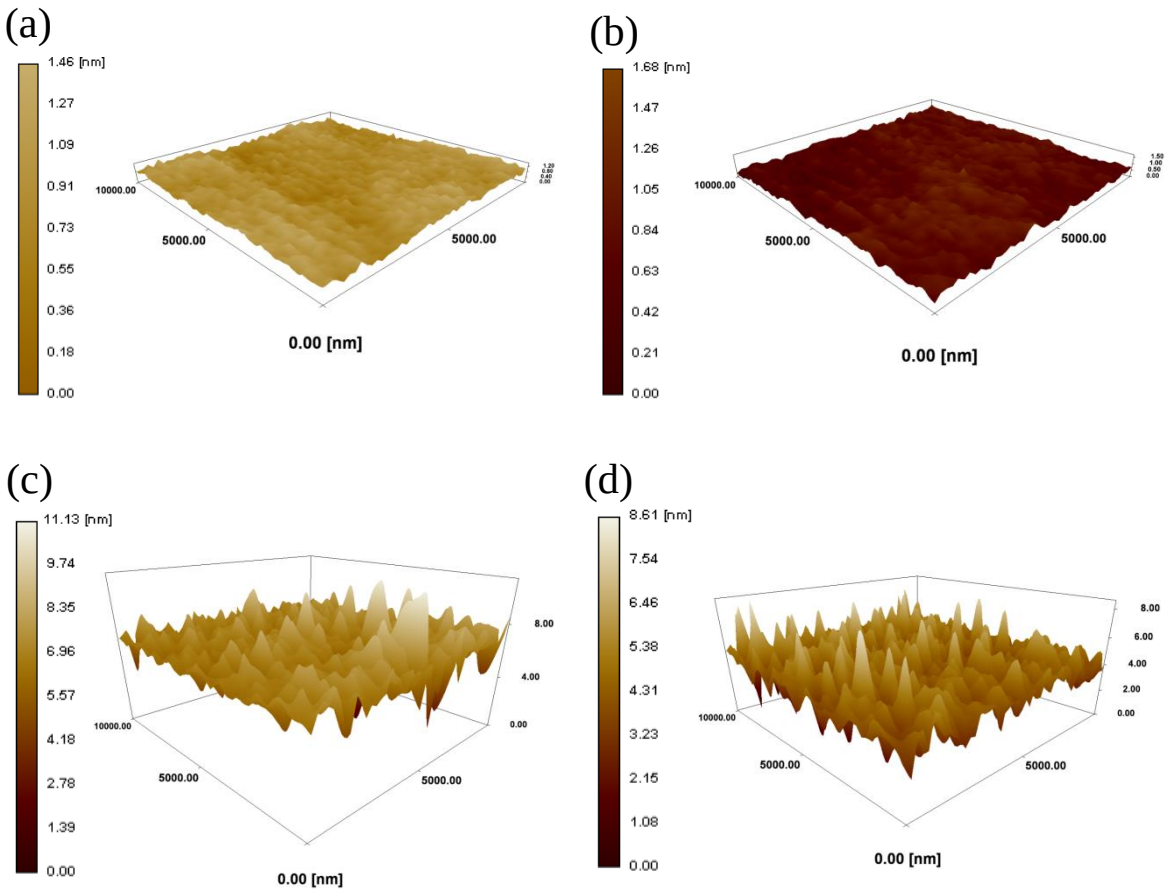


Figure S6 Dynamic force mode (DFM) of atomic force microscope (AFM) images of the bare surface and Pt-deposited surface: (a) MgO (b) $SiO_2$ (c) Pt / MgO (d) Pt / $SiO_2$ surface.

**S7. The thickness dependence of the oriented structure on the MgO surface**

Figure S7 shows the thickness dependence of the p-MAIR spectra at the MgO surface. The absorbance did not depend so much compared to the case of the Pt-deposited surface.

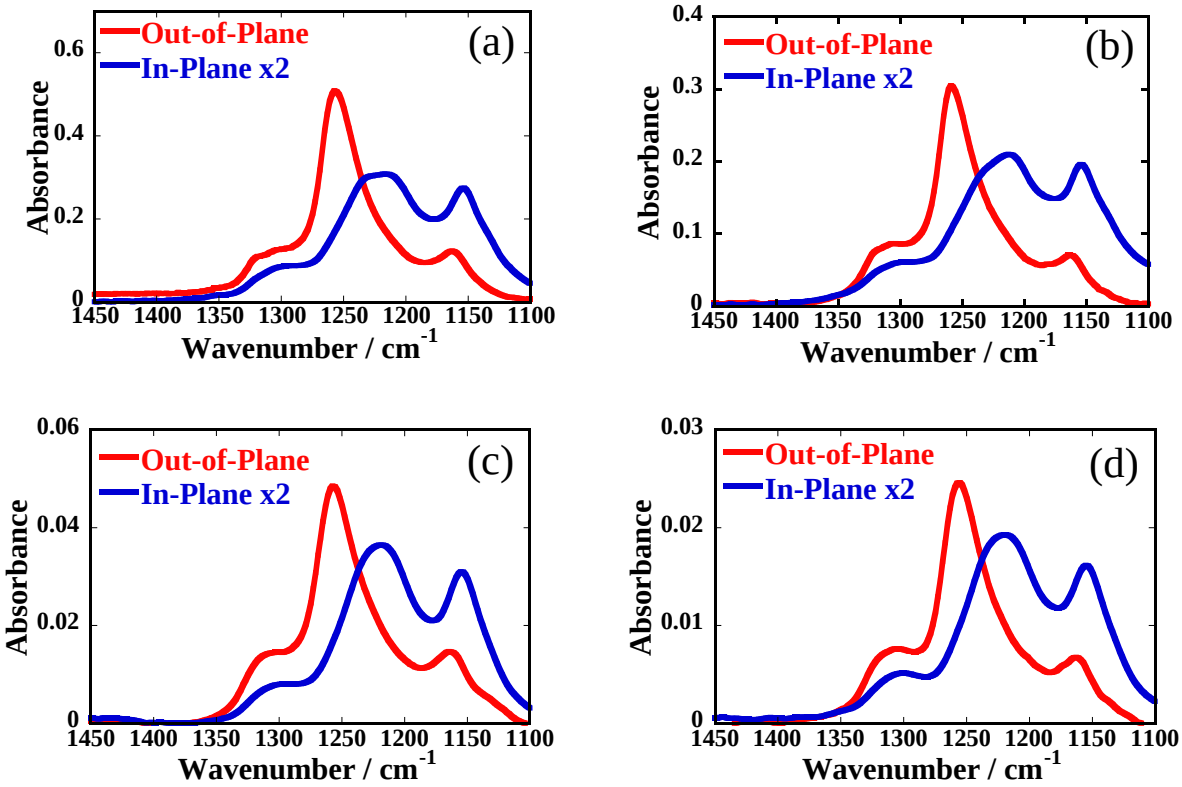


Figure S7 IR p-MAIR spectra of a Nafion thin film on the MgO surface. The thickness of Nafion thin films is (a)400 nm, (b)250 nm, (c) 30 nm, (d)20-nm-thick.

**S8. Arrhenius plots for proton conductivity at various RH**

Figure S8 shows the Temperature dependence of proton conductivities at various RH. All log($\sigma T$) lineally depended on the 1000T$^{-1}$ in this temperature region.

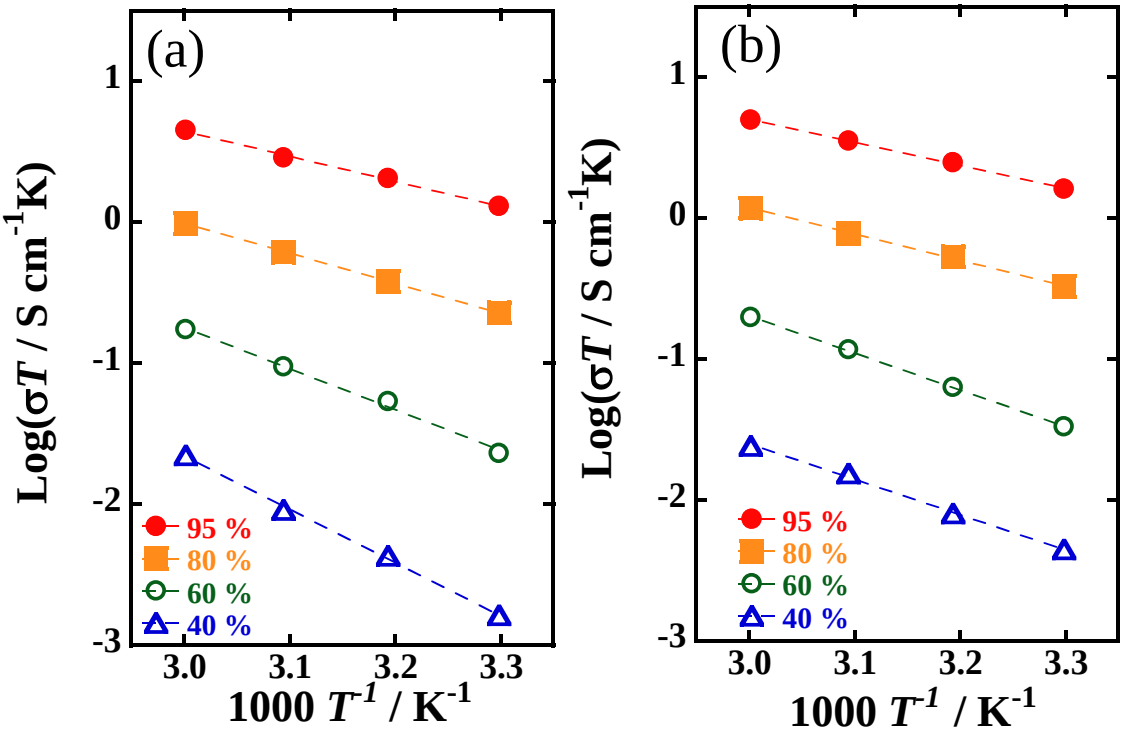


Figure S8 Temperature dependence of proton conductivities at various RH. (a) 40-nm -thick film on $SiO_2$ surface. (b) 40-nm-thick film on Pt-deposited surface.

Our observed proton conductivity was lower as compared to those reports [S2,S3]. This difference of proton conductivity may be attributed to difference of the electrode configuration or the film preparation techniques such as spin-coating, self-assembly and drop-cast.

## S9. References

[S1] Hasegawa, T. Advanced Multiple-angle Incidence Resolution Spectrometry for Thin-layer Analysis on a Low-refractive-index Substrate. *Anal. Chem.* **2007**, *79*, 4385–4389.

[S2] Modestino, M. A.; Paul, D. K.; Dishari, S.; Petrina, S. A.; Allen, F.; Hickner, M. A.; Karan, K.; Segalman, R. A.; Weber, A. Z. Self-Assembly and Transport Limitations in Confined Nafion Films. *Macromolecules* **2013**, *46*, 867–873.

[S3] Siroma, Z.; Kakitubo, R.; Fujiwara, N.; Ioroi, T.; Yamazaki, S.; Yasuda, K. Depression of Proton Conductivity in Recast Nafion Film Measured on Flat Substrate. *J. Power Sources* **2009**, *189*, 994–998.